

Thioflavin T binds dimeric parallel-stranded GA-containing non-G-quadruplex DNAs: a general approach to lighting up double-stranded scaffolds

Shuangna Liu, Pai Peng, Huihui Wang, Lili Shi* and Tao Li*

Department of Chemistry, University of Science and Technology of China, Hefei, Anhui 230026, China

Received August 10, 2017; Revised September 29, 2017; Editorial Decision October 02, 2017; Accepted October 03, 2017

ABSTRACT

A molecular rotor thioflavin T (ThT) is usually used as a fluorescent ligand specific for G-quadruplexes. Here, we demonstrate that ThT can tightly bind non-G-quadruplex DNAs with several GA motifs and dimerize them in a parallel double-stranded mode, accompanied by over 100-fold enhancement in the fluorescence emission of ThT. The introduction of reverse Watson–Crick T–A base pairs into these dimeric parallel-stranded DNA systems remarkably favors the binding of ThT into the pocket between G•G and A•A base pairs, where ThT is encapsulated thereby restricting its two rotary aromatic rings in the excited state. A similar mechanism is also demonstrated in antiparallel DNA duplexes where several motifs of two consecutive G•G wobble base pairs are incorporated and serve as the active pockets for ThT binding. The insight into the interactions of ThT with non-G-quadruplex DNAs allows us to introduce a new concept for constructing DNA-based sensors and devices. As proof-of-concept experiments, we design a DNA triplex containing GA motifs in its Hoogsteen hydrogen-bonded two parallel strands as a pH-driven nanoswitch and two GA-containing parallel duplexes as novel metal sensing platforms where C–C and T–T mismatches are included. This work may find further applications in biological systems (e.g. disease gene detection) where parallel duplex or triplex stretches are involved.

INTRODUCTION

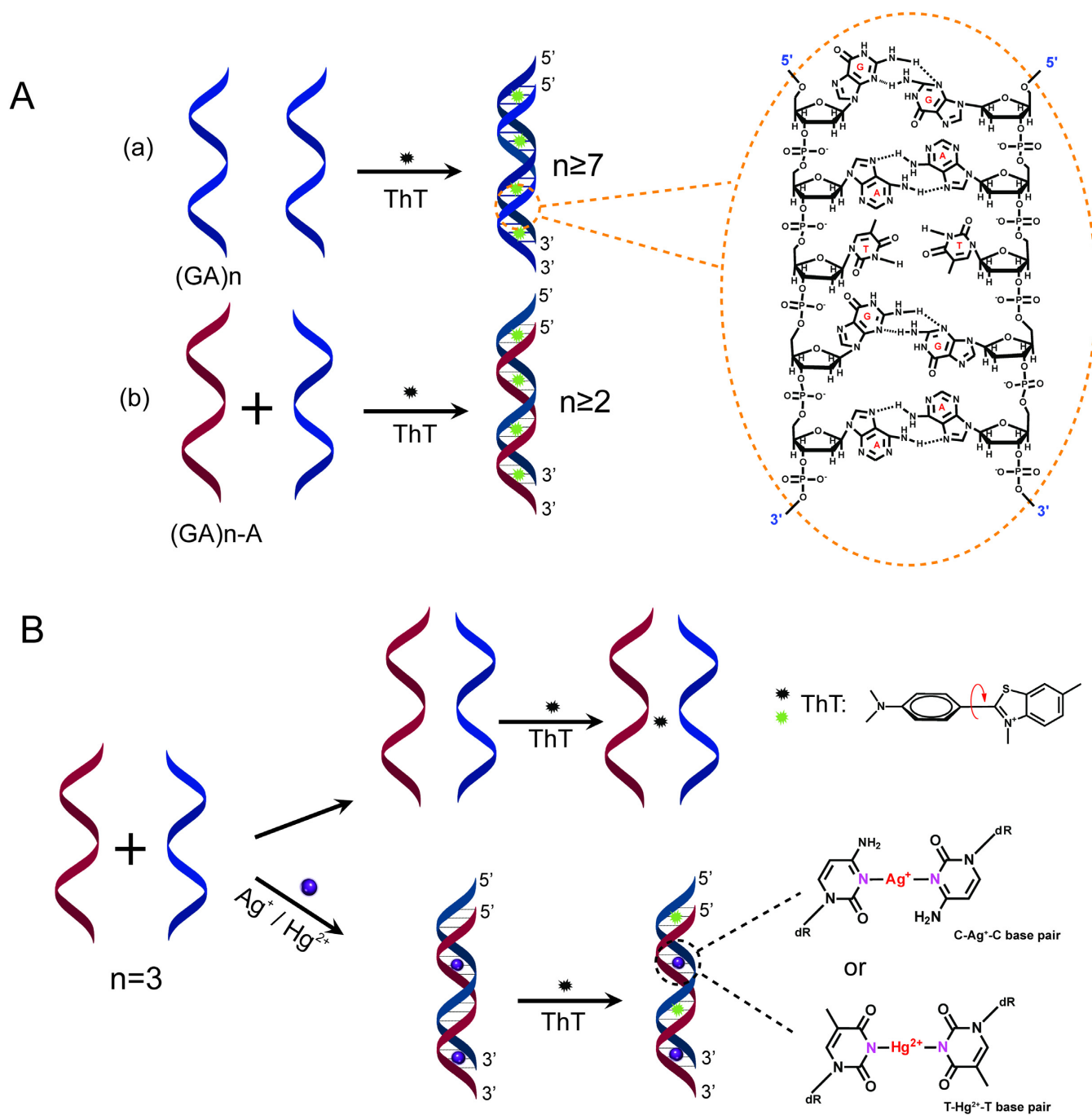
In the past years, significant effort has been devoted to finding ideal fluorescent ligands for binding and lighting up DNA structures used in a diversity of label-free biosensors and devices (1–3). Among them, thioflavin T (ThT) has recently attracted increasing interest. ThT is a molec-

ular rotor known as a fluorescent indicator for the determination of amyloid fibrils and amyloid-related diseases (4,5). Recent studies demonstrated that ThT can also bind DNA structures, accompanied by a sharp increase in fluorescence emission (6–9). Such a fluorescence enhancement of ThT results from restricting the rotation of its benzothiazole and aminobenzene rings and holding them in the same plane where the photoinduced twisted internal charge transfer and radiative transition are favored (10–12). Given the rigid structures of G-quadruplexes consisting of stacked large planar G-tetrad, the interaction of ThT with G-quadruplexes is of particular interest, as it gives rise to a bright fluorescence emission of ThT (6). This feature allows G-quadruplexes to serve as popular construction components for DNA sensors and devices based on the fluorescence enhancement character of ThT (13–17).

However, an unprecedentedly high fluorescence efficiency of ThT bound to a non-G-quadruplex DNA has been reported recently (18). In addition, some researches show that other DNA structures such as i-motifs and duplexes can enhance the fluorescence of ThT to some extent (19,20). Interestingly, we found that G is the most favorable nucleobase for ThT binding (18), implying an important role of G in ThT binding even if no G-quadruplex is formed. Hence, a systematic understanding of the interactions of ThT with non-G-quadruplex DNAs will be useful for designing new DNA-based biosensors and devices, meanwhile extending the application potential of ThT in the related fields.

Herein, we systematically investigate the interactions of ThT with some non-G-quadruplex DNAs (see Supplementary Table S1 in Supporting Information), together with several known G-quadruplexes. These DNAs are all found to remarkably enhance the fluorescence emission of ThT. Importantly, we find that the fluorescence of ThT bound to non-quadruplex DNAs is dependent on the number of GA motifs and the formation of a parallel duplex (Scheme 1A), verified by polyacrylamide gel electrophoresis (PAGE). This is further confirmed by introducing reverse Watson–Crick T–A base pairs into the DNA systems. Based on this finding, high performance sensors of Ag⁺ and Hg²⁺ are de-

*To whom correspondence should be addressed. Tel: +86 551 63601813; Email: tlliao@ustc.edu.cn
Correspondence may also be addressed to Lili Shi. Email: llshi@ustc.edu.cn



Scheme 1. Schematic for the interactions of ThT with non-G-quadruplex DNAs and their sensing applications. (A) Parallel-stranded modes for the ThT-induced homo-dimer of $(GA)_n$ (a) and the hetero-dimer formed by $(GA)_n$ and $(GA)_{n-A}$ (b). The homo-dimer is mainly stabilized by $G \bullet G$ and $A \bullet A$ base pairs separated by T-T mismatches, whereas the T-T mismatches are replaced by reverse Watson-Crick T-A base pairs in the hetero-dimer. A molecular structure unit of the homo-dimer of $(GA)_8$ is proposed according to previous studies (25,26). (B) Lighting up a parallel duplex-based metal sensing platform with ThT. Here several C-C and T-T mismatches are employed to replace reverse Watson-Crick T-A base pairs, enabling the fluorescent detection of Ag^+ and Hg^{2+} , respectively.

signed via introducing several C–C or T–T mismatches into such parallel double-stranded systems, the stability of which is improved by the formation of C–Ag⁺–C or T–Hg²⁺–T pairs (21,22). In addition, a pH-switched triplex system with good signal readout and reversibility was also successfully constructed.

MATERIALS AND METHODS

Oligodeoxynucleotides and chemicals

Oligodeoxynucleotides (see Supplementary Table S1 in Supporting Information) were synthesized by Sangon Biotechnology (Shanghai, China), and used directly without further purification. All were dissolved in 10 mM Tris–EDTA buffer (pH 8.0) as stock solutions and determined by ultraviolet (UV) spectrometry using the extinction coefficient ($\epsilon_{260\text{ nm}}$, $\text{M}^{-1}\text{cm}^{-1}$). The stock solutions were stored in a refrigerator at 4°C before use. Thioflavin T was purchased from Sigma-Aldrich (USA). Magnesium acetate (MgAc_2), silver nitrate (AgNO_3) and mercury acetate (HgAc_2) were obtained from Energy Chemical. All chemical reagents were of reagent grade and used without further purification.

Before all experiments, all DNAs were diluted to 40 mM TA (Tris–Ac, pH 8.0) buffer to desired concentrations and heated at 90°C for 10 min and cooled down to room temperature gradually.

Fluorescence spectra & fluorometric titration

For every sample, 1 μM (total concentration) DNA was prepared in 40 mM TA buffer (pH 8). In exploration experiments, 50 μM ThT was added to the above solution at room temperature. In application experiments, meanwhile, 5 μM ThT was added at 15°C. After 5 min reaction, fluorescence spectra was collected on a Hitachi F-4600 Fluorescence spectrometer (Tokyo, Japan) with an excitation wavelength at 442 nm and scanning emission wavelength range from 455 to 650 nm.

Fluorometric titration was performed by monitoring fluorescence spectra of 0.1 μM ThT with the concentration of DNA varying from 0.1 to 100 μM using the F-4600 Fluorescence spectrometer at the excitation wavelength of 442 nm and fluorescence intensity at 492 nm was used to plot the titration curve. The binding constants were calculated from previous studies (23,24).

Native PAGE

Non-denaturing polyacrylamide gel (18%) was used for 5 μM DNA prepared in the TA buffer (pH 8) in the absence or presence of 50 μM ThT. Gel electrophoresis was run in the same buffer under a voltage of 4 V/cm at 4°C for 14 h. Then the gel was stained in 0.01% Stains-All solution for 4 h and destained in deionized water under light until bands became clear, finally photographed with a camera.

Circular dichroism (CD) study

The CD spectra of 25 μM oligodeoxynucleotides in TA buffer (pH 8) in the absence or in 50 μM ThT were

measured with a Jasco J-1500 spectropolarimeter (Tokyo, Japan) at 4°C. Three scans from 210 to 320 nm with a rate of 100 nm/min were accumulated and averaged. In each case, the background of the buffer solution was subtracted from the CD data.

The CD melting curves at the positive peak of each CD spectrum were recorded with a rate of 1°C/min. The CD signal was normalized in each case. The T_m value of DNA was obtained at which 50% of parallel double strand structures were dissociated.

RESULTS

Interactions of ThT with non-quadruplex DNAs

To easily understand how ThT interacts with non-quadruplex DNAs, we chose the known human telemetric DNA, GGGTTA, as the target, and varied its sequence to obtain some variants. For more details, see Supplementary Table S1 in Supporting Information. Figure 1A shows that all of the DNA variants noticeably enhance the fluorescence emission of ThT, as compared to the duplexes ds-AT and ds-CG. In particular, some non-G-quadruplex DNAs (e.g. GATGAT and GAGTTA) behave as stronger enhancers for ThT than the reference G-quadruplex DNAs T30695 and TBA. We further employed CD spectra to reveal the dominant structures of these DNAs induced by ThT (Figure 1B). T30695 and ATTGGG both display a positive peak around 260 nm and a negative one near 240 nm, consistent with the typical CD characteristic of parallel G-quadruplexes (27,28). In contrast, TBA and GGGTTA show a CD characteristic of antiparallel G-quadruplexes, with a positive peak around 290 nm and a negative one near 260 nm (28). Surprisingly, the non-G-quadruplex DNA GATGAT also exhibits a CD characteristic of parallel G-quadruplexes. This is possibly attributed to a ThT-induced arrangement of all G residues at the *anti* position like in parallel G-quadruplexes (29). In fact, this unusual phenomenon has been observed in the CD spectrum of the ATP-aptamer complex (18), which adopts a hairpin-like secondary structure confirmed by nuclear magnetic resonance (30).

The unusual behaviors of GATGAT are also observed in gel electrophoresis (Figure 1C). In the absence and presence of ThT, this non-G-quadruplex DNA always has an electrophoretic mobility very close to those of two duplexes ds-AT and ds-CG (lane 8 versus lanes 10, 11), suggesting the dimerization of GATGAT. In the presence of ThT, GGATTA displays an electrophoretic behavior similar to that of GATGAT (Figure 1C, bottom panel, lane 5 versus lane 8), indicating the formation of a dimer rather than a G-quadruplex induced by ThT. Without ThT, this DNA is mainly in the single-stranded state (Supplementary Figure S1 in Supporting Information, and Figure 1C, top panel, lane 5). The other three non-G-quadruplex DNAs GAGTTA, GAGATT and TAGTAG are mainly in the single-stranded state independent of ThT (Figure 1C, lanes 6, 7, 9), although ThT can induce a small amount of GAGATT to form a dimer reflected by a faint band moving slowly like that of GATGAT (Figure 1C, bottom panel, lane 7). In the presence of ThT, GGGTTA moves a little faster than single strands while ATTGGG moves slightly slower

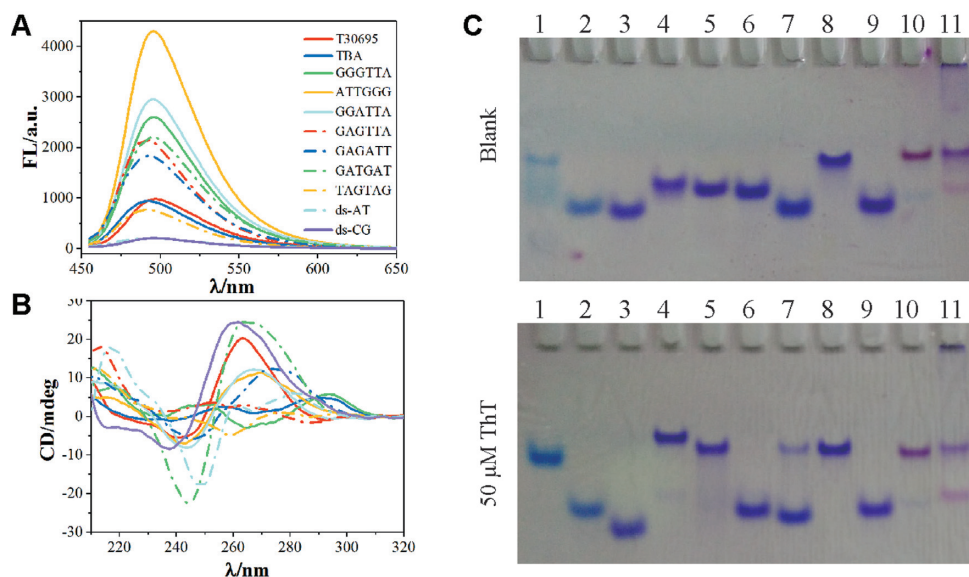


Figure 1. Investigation of the interactions of ThT with different DNAs. (A) Fluorescence spectra of ThT (50 μ M) incubated with different DNAs. (B) CD spectra of different DNA systems shown in Figure 1A. (C) Gel electrophoretograms of DNAs in the absence or presence of 50 μ M ThT. Lanes 1–11: T30695, TBA, GGGTTA, ATTGGG, GGATTA, GAGTTA, GAGATT, GATGAT, TAGTAG, ds-AT and ds-CG.

than duplexes (lanes 3, 4), consistent with their antiparallel and parallel quadruplex structures indicated by CD spectra.

The above observations clearly demonstrate that, like G-quadruplexes, some non-G-quadruplex DNAs can efficiently enhance the fluorescence emission of ThT under appropriate conditions. This is mainly attributed to the existence of G residues who play an important role in ThT binding (18) (also see Supplementary Figure S2 in Supporting Information). However, it cannot explain the large differences in the fluorescent and electrophoretic behaviors of GATGAT and TAGTAG with the same number of G. Apparently, the adjacent nucleobases around G also have a significant influence on ThT binding to these non-G-quadruplex DNAs.

A GA-containing parallel double-stranded mode for ThT binding

By comparing the sequences of non-quadruplex DNAs tested here, we found most of them contain several GA motifs, except for TAGTAG that displays a much lower enhancement on ThT fluorescence than other sequences (Figure 1A). Hence, we hypothesized that GA may be most favorable motif for ThT binding to non-G-quadruplex DNAs. To demonstrate it, we investigated the interactions of ThT with two groups of non-G-quadruplex DNAs of the same sequence length. In one group, we varied the number of GA motif from one to eight, while in another group eight GA motifs are replaced by AG, GC, GG or GT, respectively. Figure 2A shows that the fluorescence intensity of ThT obviously increases with the number of GA, reflecting an important role of GA in ThT binding. Furthermore, the GA motif is found to give the highest enhancement of the fluorescence of ThT compared to others (Figure 2A, insert), confirming GA as the best motif for ThT binding in non-G-quadruplex DNAs. Meanwhile, trinucleotide motifs (GGA,

GGG, GAG, etc.) are also compared briefly (see Supplementary Figure S3 in Supporting Information).

From Figure 2A we notice that the fluorescence intensity of ThT ascends slowly by varying the number of GA from one to five. However, a sharp rise in the fluorescence is observed when the GA number is beyond six, attributed to the formation of a dimer verified by native PAGE (Figure 2B). In the absence and presence of ThT, (GA)₈ can always form a stable dimer (Figure 2B, lane 12), while the dimerization of (GA)₇ is clearly observed only in the presence of ThT (bottom panel, lane 11). A smiling band of (GA)₆ appears, induced by ThT, implying the formation of an unstable dimer under electrophoretic conditions (lane 10). In each case, no dimers of (GA)_{1–5} are found. It is found that the DNA band moves faster and faster as the GA number increases from one to six (lanes 5–10). This unusual phenomenon can be explained by big differences between the electrophoretic mobility of poly-A, poly-C, poly-G and poly-T (top panel, lanes 1–4). Under same conditions, poly-T has a much slower mobility than others, although it is mainly in the single-stranded state (see Supplementary Figure S4 in Supporting Information). In the sequences of (GA)_n, the number of T decreases as the GA number increases. As a consequence, those single strands (i.e. (GA)_{1–5}) with more GA motifs move faster.

Likewise, the dimerization of non-G-quadruplex DNAs can also explain the differences in their fluorescence intensity (Figure 2A, insert). (GC)₈ and (AG)₈ are mainly in the single-stranded state verified by PAGE (Figure 2B, lanes 14, 16) and CD (Figure 2C), and so have a lower enhancement on the fluorescence of ThT. So does (GT)₈, although it moves slowly owing to the existence of a large amount of T (lane 15). Induced by ThT, (GG)₈ can form a parallel G-quadruplex (lane 13), and it has a moderate enhancement of ThT fluorescence.

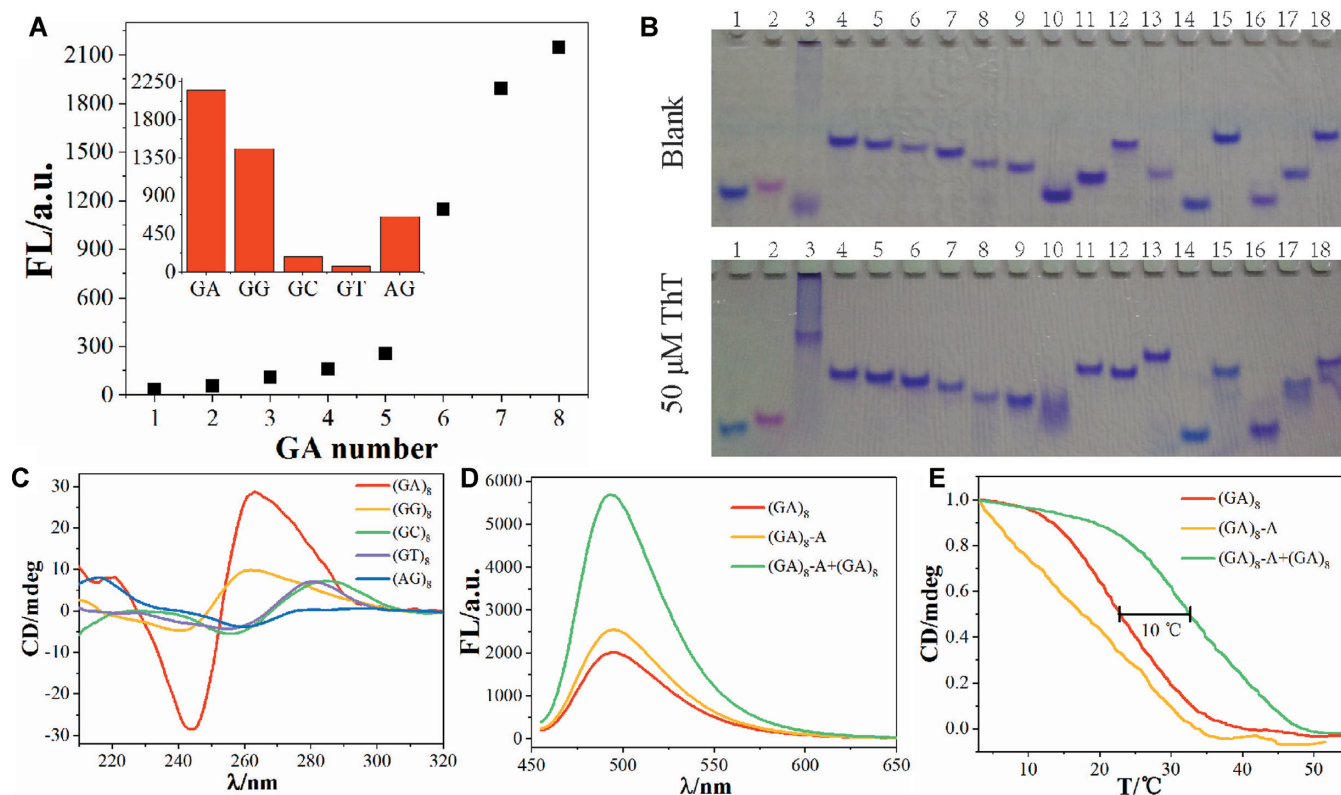


Figure 2. Investigation of ThT binding to different non-G-quadruplex DNAs. (A) Fluorescence intensity at 492 nm of 50 μM ThT in the presence of $(\text{GA})_n$ ($n = 1-8$). The inset shows a comparison between $(\text{GA})_8$, $(\text{AG})_8$, $(\text{GC})_8$, $(\text{GG})_8$ and $(\text{GT})_8$. (B) Electrophoretograms of DNA in the absence or presence of 50 μM ThT. Lanes 1–4: poly-A, poly-C, poly-G, poly-T; Lanes 5–12: $(\text{GA})_1$, $(\text{GA})_2 \dots (\text{GA})_8$; Lanes 13–18: $(\text{GG})_8$, $(\text{GC})_8$, $(\text{GT})_8$, $(\text{AG})_8$, $(\text{GA})_8\text{-A}$, $(\text{GA})_8 + (\text{GA})_8\text{-A}$. (C) CD spectra of $(\text{GA})_8$, $(\text{AG})_8$, $(\text{GC})_8$, $(\text{GG})_8$ and $(\text{GT})_8$ together with 50 μM ThT. (D) Fluorescence spectra of ThT of $(\text{GA})_8$, $(\text{GA})_8\text{-A}$ and the mix of $(\text{GA})_8$ and $(\text{GA})_8\text{-A}$. (E) CD melting curves of $(\text{GA})_8$, $(\text{GA})_8\text{-A}$ and their mixture, respectively. The CD signal was normalized in each case.

We then endeavored to figure out the reason for the dimerization of these non-G-quadruplex DNAs. Since the dimers of $(\text{GA})_n$ become more stable when n value increases from six to eight (Figure 2B, lanes 10–12), these dimers most possibly adopt a parallel double-stranded structure rather than an antiparallel one because $\text{G}\bullet\text{G}$ and $\text{A}\bullet\text{A}$ base-pairing can efficiently stabilize parallel duplexes (31,32). Meanwhile, the replacement of GA by GC or GT reduces the base pairs that stabilize parallel duplexes, resulting in no formation of dimers. In contrast, GG replacing GA still allows the dimer to keep stable. To further confirm the formation of a parallel duplex by $(\text{GA})_8$, we introduced additional reverse Watson–Crick T–A base pairs to stabilize parallel duplexes (33) via hybridizing $(\text{GA})_8$ with another sequence $(\text{GA})_8\text{-A}$, which is obtained by replacing all T of $(\text{GA})_8$ by A. Figure 2B shows that the duplex formed by $(\text{GA})_8$ and $(\text{GA})_8\text{-A}$ is stable even in the absence of ThT (lane 18). Compared with $(\text{GA})_8$ and $(\text{GA})_8\text{-A}$ alone, this duplex displays a more excellent enhancement of the fluorescence of ThT (Figure 2D), even higher than the best G-quadruplex ATTGGG tested here (green curve, Figure 2D versus Figure 1A) and previously reported ABA27 (18) (see Supplementary Figure S5 in Supporting Information). Under this condition, an affinity for ThT binding ($K_d \sim 14 \mu\text{M}$) can be obtained (23,24), much higher than those of $(\text{GA})_8$ and $(\text{GA})_8\text{-A}$ (see Supplementary Figure S6 in supporting informa-

tion). In addition, ThT binds to ATTGGG with an affinity ($K_d \sim 45 \mu\text{M}$), which is also lower than that of the duplex. Thermal denaturation indicates an over 10°C increment in the melting temperature of the duplex after adding reverse Watson–Crick T–A base pairs (Figure 2E). These observations strongly suggest that a parallel double-stranded mode is favorable for ThT binding to $(\text{GA})_8$ and other tested non-G-quadruplex DNAs. Previous studies demonstrated that the A residues in parallel-stranded poly-A are all at the *anti* position (26), whereas the G residues in parallel duplexes can be at the *syn* or *anti* position (25). However, the CD spectrum of the dimeric $(\text{GA})_8$ (Figure 2C), which is similar to that of parallel G-quadruplexes (27,28), suggests that all G residues are located at the *anti* position in the presence of ThT. Accordingly, a molecular structure of dimeric parallel-stranded $(\text{GA})_8$ is proposed, as shown in Scheme 1A.

To demonstrate this issue more clearly, we designed two groups of parallel and antiparallel GA-containing duplexes, $(\text{GA})_n\text{-ps}$ and $(\text{GA})_n\text{-aps}$ ($n = 3-5$). Under identical conditions, $(\text{GA})_n\text{-ps}$ displays a far higher enhancement of ThT fluorescence than $(\text{GA})_n\text{-aps}$ (Figure 3A), although the latter also gives rise to an obvious increase in fluorescence when the GA number increases to five. Apparently, a parallel mode is predominant in the interactions of ThT with GA-containing duplexes.

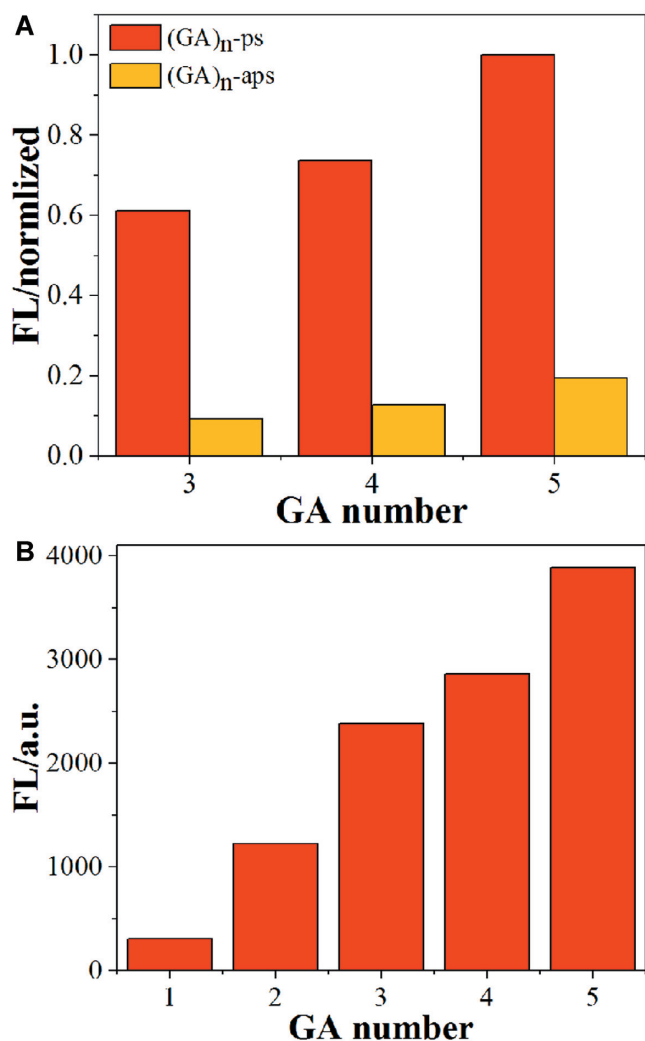


Figure 3. Validation of the parallel-stranded dimeric mode for non-G-quadruplex DNAs bound by ThT. (A) Fluorescence intensity of 50 μM ThT at 492 nm in the presence of (GA)_n-ps and (GA)_n-aps ($n = 3-5$). (B) Fluorescence intensity of 50 μM ThT in the presence of (GA)_n-ps ($n = 1-5$). Total DNA concentration is 1 μM .

We noticed that such a parallel duplex stabilized by reverse Watson–Crick T–A base pairs only needs a few GA motifs to dramatically enhance the fluorescence of ThT (Figure 3B), unlike (GA)_n shown in Figure 2A. It means that more GA motifs (>3) of (GA)₆₋₈ in Figure 2 mainly help to stabilize their dimeric parallel-stranded structures by G•G and A•A base-pairing, but do not significantly influence ThT binding. This allows us to adopt a minimal number of GA motifs (e.g. $n = 3$) to design parallel double-stranded platforms for sensing applications (vide infra). In such a DNA system, GA still is the best motif to promote the fluorescence of ThT as compared with others (Figure 4A). In contrast, AG has a little enhancement on ThT fluorescence, attributed to lowering the structural stability in case of replacing GA by AG in the duplex (34,35) (see Supplementary Figure S7 in Supporting Information). In fact, this duplex cannot remain stable under electrophoretic conditions, as shown in Figure 4B (lane 7). Figure 4A shows

that GG is also a good motif for ThT binding in this type of parallel duplex, and efficiently stabilizes the duplex (Figure 4B, lane 5). In other cases, the duplexes are virtually absent (lanes 3, 4, 8). These observations are consistent with those in Figure 2. Based on the results, we rationally deduce that the G•G base pair followed by an A•A (or G•G) pair in a parallel double-stranded DNA scaffold can provide an active pocket to encapsulate ThT, where the ThT molecule interacts with two adjacent base-pairs via π – π stacking (Figure 4C). As a consequence, the two rotatory aromatic rings of ThT are restricted in the excited state, thereby promoting its fluorescence emission. We further verified this proposed structural mode via replacing the secondary A•A pair by a reverse Watson–Crick T–A base pair (see Supplementary Figure S8A in Supporting Information). In this case, ThT does not tightly bind the parallel duplex and no enhanced fluorescence is observed (Supplementary Figure S8B).

Parallel duplex-based metal sensors

Since the binding of ThT to GA-containing parallel duplexes is dependent on the stability of the secondary structure, we next sought to employ some external stimuli (e.g. metal ions) to modulate the formation of parallel duplexes (36). As we know, Ag⁺ can specifically interact with the C–C mismatches in a DNA duplex and improve the structural stability via the formation of C–Ag⁺–C base pairs (21,37,38). Accordingly, a novel fluorescent Ag⁺ sensor is here constructed by introducing four C–C mismatches into the parallel duplex (GA)₃-ps, whose fluorescence enhancement is highest after being assembled into parallel duplexes (see Supplementary Figure S9 in Supporting Information). Figure 5A shows that, in the absence of Ag⁺, the two mixed strands only cause a very low background fluorescence from ThT, attributed to the existence of C–C mismatches that destroy the parallel duplex. Upon addition of Ag⁺, the formation of C–Ag⁺–C base pairs help to stabilize the parallel duplex that binds ThT tightly, reflected by a significant increase in the fluorescence intensity of ThT. The plot of the fluorescence intensity at 492 nm versus Ag⁺ concentration shows that 50 nM Ag⁺ can lead to an observable change in the fluorescence intensity (Figure 5B), indicating a limit of detection (50 nM) for Ag⁺ detection with a linear relationship in the range of 0.05–2 μM (Figure 5B, insert). To evaluate the specificity of this sensor, the selectivity over other counterparts was tested by employing other metal ions (Li⁺, Na⁺, K⁺, Mg²⁺, Cu²⁺, Zn²⁺, Mn²⁺, Pb²⁺ and Hg²⁺) in place of Ag⁺ to perform parallel measurements. Figure 5C shows that most of tested metal ions have little influence on the analysis of Ag⁺, indicating a good selectivity of our developed Ag⁺ sensor.

Likewise, by introducing several T–T mismatches into the parallel duplex (GA)₃-ps, this system can be utilized to detect Hg²⁺ owing to the T–Hg²⁺–T interaction (22,39,40) that stabilizes the duplex. Figure 5D indicates that the fluorescence of ThT increases with increasing Hg²⁺ concentration. It is observed that 50 nM Hg²⁺ can cause a noticeable change in the fluorescence, namely, a detection limit of 50 nM for Hg²⁺ analysis is achieved (Figure 5E), with a linear relationship in the range of 50–800 nM (Figure 6E, insert).

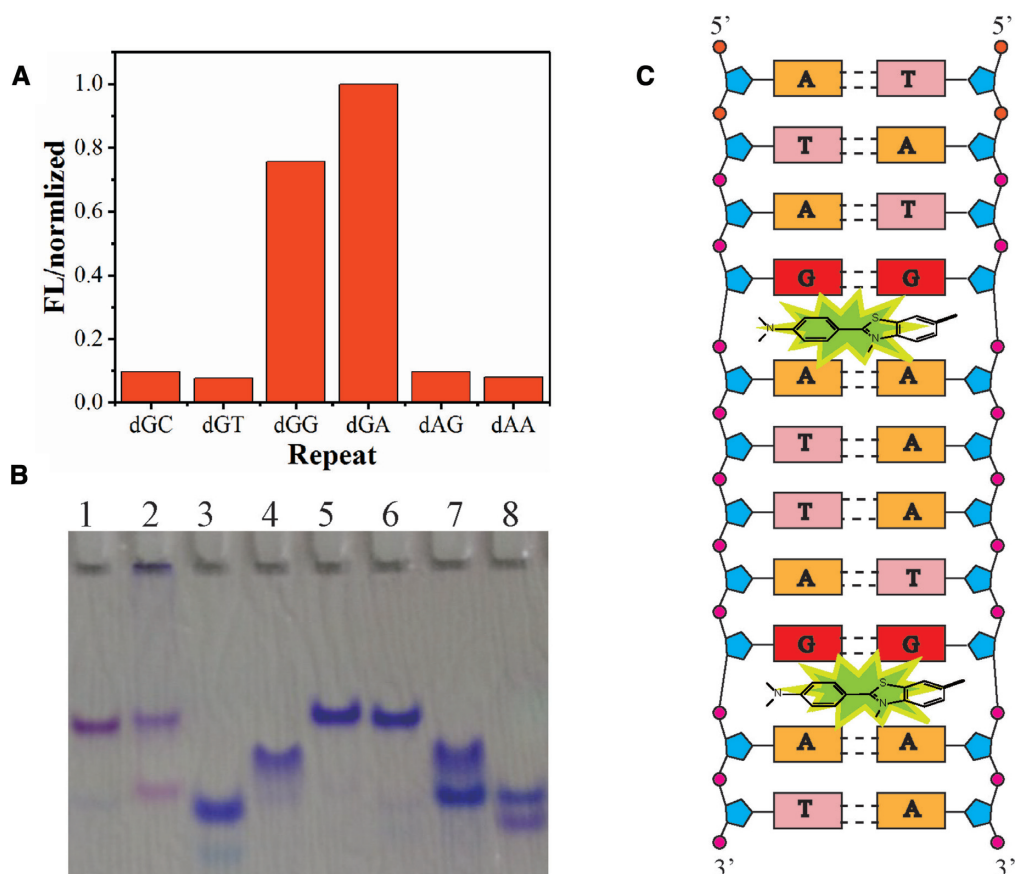


Figure 4. The binding site of ThT to parallel duplex. (A) Fluorescence intensity of 50 μM ThT in the presence of parallel duplexes containing three repeat of GC, GT, GG, GA, AG and AA, respectively. (B) Gel electrophoretograms of DNA systems corresponding to panel A. Lanes 1–8: ds-AT, ds-CG, GC, GT, GG, GA, AG and AA. (C) Proposed structural mode for the interaction of ThT with the GA-containing parallel duplex.

The specificity of this Hg^{2+} sensor was also tested, indicating a good selectivity over other metal ions (Figure 5F).

To test the practicality of our developed metal sensors, we applied them to analyzing the real freshwater samples (lake water). It is found that the concentrations of Ag^+ and Hg^{2+} in real samples are too low to cause an obvious change in fluorescence signal. By adding the metal ions into the working system, the metal-concentration-dependent change of fluorescence intensity is observed (see Supplementary Figure S10 in Supporting Information). In this case, 100 nM Ag^+ and 50 nM Hg^{2+} can cause an obvious change in signal readout, indicating that potential interferents in real environmental samples have little influence on the sensitivity of these sensors.

Note that the above metal sensors are built on the formation of parallel duplexes that are usually less stable than antiparallel ones. Introducing several C–C or T–T mismatches into the duplex further lowers the structure stability, while it is necessary for specifically probing Ag^+ or Hg^{2+} . Such a compromise mainly accounts for a relatively low sensitivity as compared with previous counterparts (41).

pH-driven triplex switch

Besides parallel duplexes, an antiparallel triplex also has two adjacent parallel strands stabilized by Hoogsteen hy-

drogen bonds (42). In particular, triplexes have been shown to play an important role in a variety of biological processes including DNA transcription and replication, gene expression, etc (42–44). With this in mind, we endeavored to determine whether ThT can be employed as an indicator for triplex formation to expand the toolbox for investigations of these biological processes.

Based on the insight into the ThT binding to GA-containing parallel duplexes, we designed a pH-switched triplex system consisting of a hairpin DNA and a third strand, with several GA motifs incorporated into the third strand and the 5' part of the hairpin (Figure 6A). The triplex is mainly stabilized by C–G•C⁺ and T–A•T triplets and therefore dependent on acidic pH (45). For this reason, its formation and dissociation can be controlled by switching the pH between 5.5 and 8 (46), verified by native PAGE (Figure 6B, lane 4). After incorporating GA motifs into the triplex, the structure still keeps stable in acidic conditions (top panel, lane 5 versus lane 4). This allows the GA motifs in the triplex structure to serve as active pockets for binding ThT and remarkably enhancing its fluorescence (Figure 6C), just like in parallel duplexes. In contrast, the components of the triplex give only a relatively low background fluorescence under the same conditions. As a consequence, the formation and dissociation of the triplex can be monitored by the fluorescence readout of ThT, as shown in Fig-

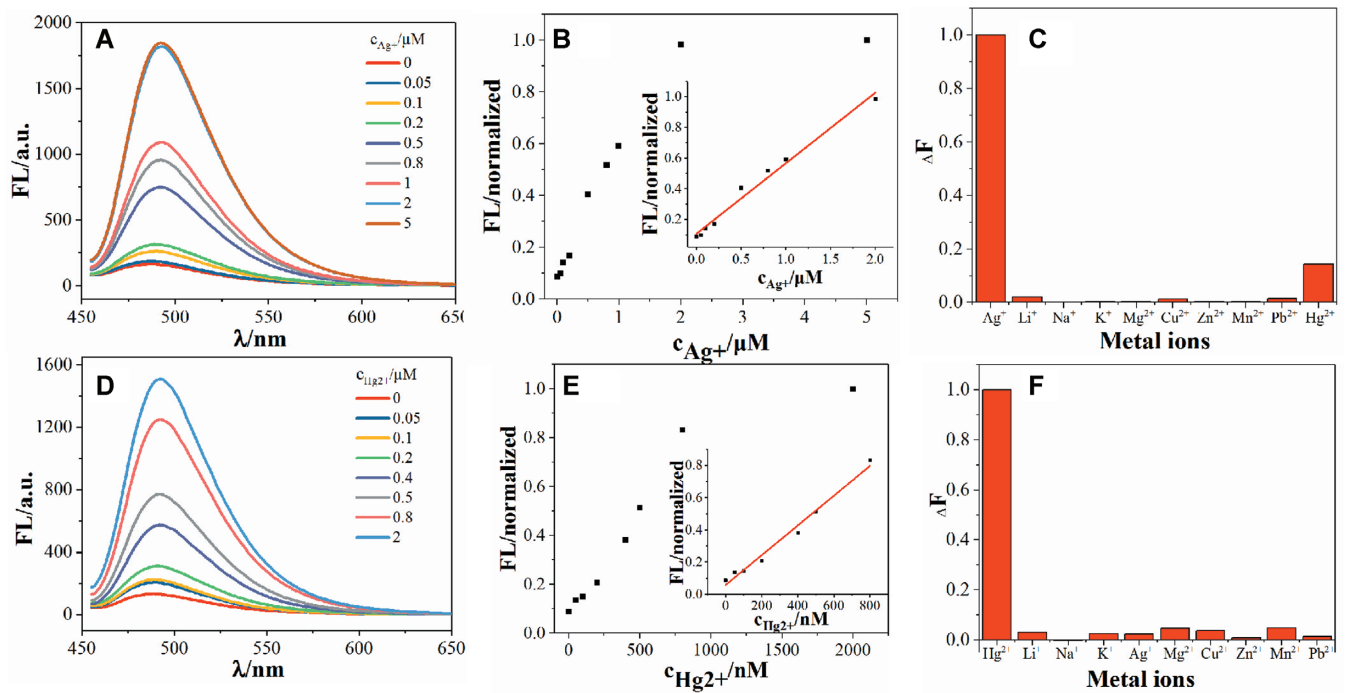


Figure 5. Silver ion and mercury ion sensors developed on the parallel duplex stabilized by C–Ag⁺–C base-pairing and T–Hg²⁺–T base-pairing. (A) Fluorescence spectra corresponding to adding different concentrations of Ag⁺ (from bottom to top) into the DNA system. (B) Plot of fluorescence intensity at 492 nm versus concentration of Ag⁺. Inset: Calibration curve in the range of 0.05–2 μ M. (C) Selectivity studies in the presence of 2 μ M Ag⁺ or Li⁺, Na⁺, K⁺, Mg²⁺, Cu²⁺, Zn²⁺, Mn²⁺, Pb²⁺, Hg²⁺, respectively. (D) Fluorescence spectra corresponding to adding different concentrations of Hg²⁺ (from bottom to top: 0–2 μ M) into the DNA system. (E) Plot of fluorescence intensity at 492 nm versus concentration of Hg²⁺. Inset: Calibration curve in the range of 0–800 nM. (F) Selectivity studies in the presence of 2 μ M Hg²⁺ or Li⁺, Na⁺, K⁺, Ag⁺, Mg²⁺, Cu²⁺, Zn²⁺, Mn²⁺, Pb²⁺, respectively.

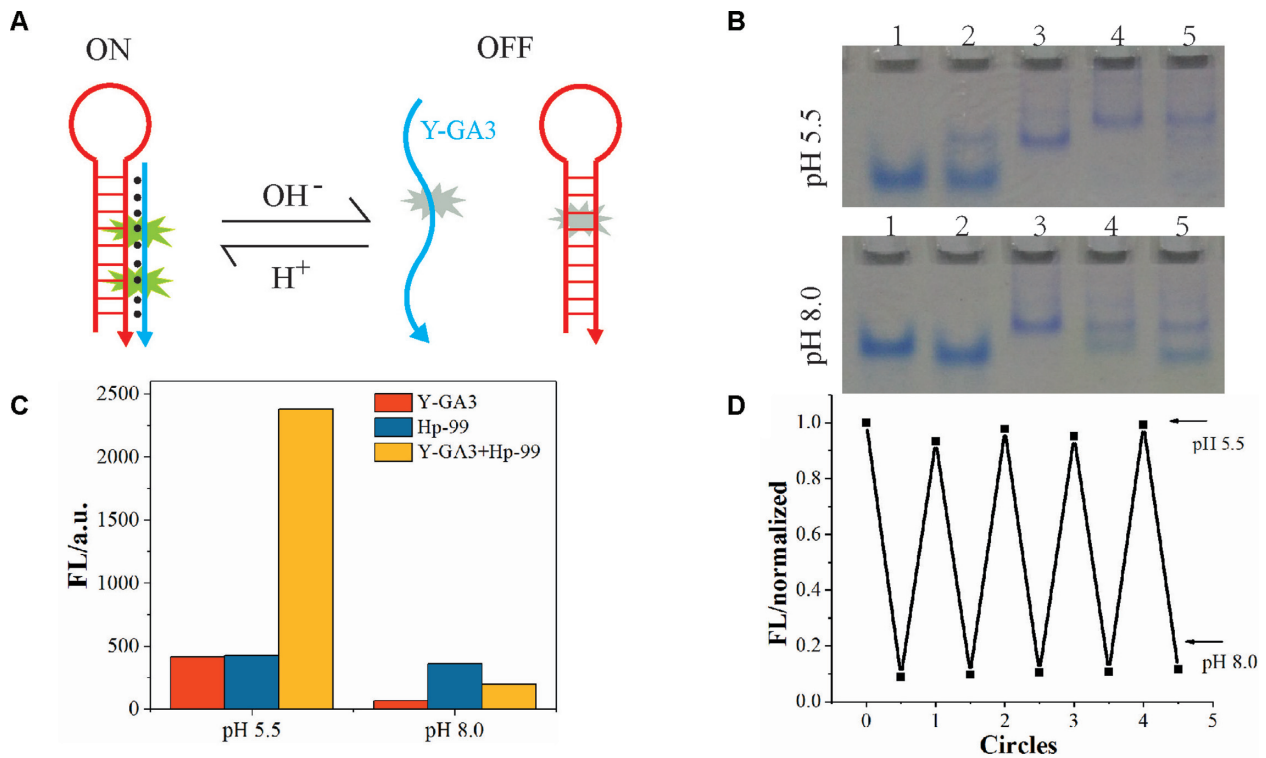


Figure 6. Interactions of ThT with DNA triplexes. (A) Schematic for a pH-driven triplex switch. (B) Gel electrophoretograms of different DNA (0.5 μ M) in pH 5.5 or pH 8.0 TA buffer with 20 mM MgAc₂. Lanes 1–5: YC; Y-GA3; Hp-99; YC + Hp-99; Y-GA3 + Hp-99. (C) Fluorescence intensity at 492 nm of 50 μ M ThT with 1 μ M DNA in pH 5.5 or pH 8.0. (D) Switching performance of the pH switch between ‘ON’ and ‘OFF’ state. The pH value was switched between pH 5.5 and 8 by alternate addition of 0.4% (v/v) 6 M HCl and 6 M NaOH. After each pH switch, the system was incubated at 37°C for 30 min.

ure 6C. Such a DNA switch can operate many times in a fully reversible fashion (Figure 6D).

DISCUSSION

We have investigated the interactions of ThT with different non-G-quadruplex DNAs, and demonstrated that those with enough GA motifs are subject to dimerizing in a parallel double-stranded mode induced by ThT. In this DNA scaffold, the ThT molecule is thought to bind the active pocket between G•G and A•A base pairs, where its two rotary aromatic rings are restricted in the excited state. Consequently, the fluorescence emission of ThT is enhanced over 100-fold, providing a novel approach to lighting up DNA-based sensors and devices. Based on this, we have designed two GA-containing parallel duplex-based sensing platforms, of which the binding of ThT to the duplex is modulated by the formation of C–Ag⁺–C or T–Hg²⁺–T base pairs. This is reflected by a sharp change in the fluorescence intensity of ThT upon addition of Ag⁺ or Hg²⁺. In this way, the detection of Ag⁺ and Hg²⁺ at nanomolar level was achieved. ThT is further utilized to indicate the pH-dependent formation of a DNA triplex, enabling the construction of a proton-fueled triplex switch.

Note that the ATP aptamer also contains several GA and GG motifs, binds ThT tightly, and remarkably enhances its fluorescence emission (18). However, this DNA aptamer forms an intramolecular structure rather than a parallel-stranded dimer in the presence of ThT (see Supplementary Figure S11A in Supporting Information), mainly attributed to the formation of a stable hairpin-like structure held by canonical G–C and T–A base pairs and a few wobble base pairs (Supplementary Figure S11B). This phenomenon illustrates the possibility for the ThT molecule to bind antiparallel duplexes or DNA hairpins with several special motifs. To demonstrate this, we tested a series of antiparallel duplexes containing a G•G wobble base pair followed by a G–X (X = A, C, G, T) pair, and compared them with the full double-stranded structures (Supplementary Figure S11C). In this case, high fluorescence of ThT is observed if two consecutive G•G wobble base pairs exist in the antiparallel duplexes, which can keep the duplex more stable than others (Supplementary Figure S11D). Likewise, the ThT molecule is proposed to be encapsulated in the pocket between two G•G wobble base pairs (Supplementary Figure S11E), where ThT is kept in the excited state.

Our study provides insight into the interactions of ThT with both parallel and antiparallel duplexes and demonstrates how to harness this knowledge for the construction of DNA molecular devices. In particular, the binding of ThT to antiparallel duplexes will provide a widely used approach to signal readout when constructing a wide range of DNA molecular devices in double-stranded scaffolds. Given that parallel duplex stretches exist in human genes related to some diseases (47), this insight may find further applications in the detection and diagnosis of disease genes. In addition, it may also be applicable to triplexes involved in a variety of biological processes (42–44,48).

SUPPLEMENTARY DATA

Supplementary Data are available at NAR online.

ACKNOWLEDGEMENTS

We thank Prof. Zachary J. Smith of the University of Science and Technology of China for reading and revising the manuscript.

FUNDING

National Natural Science Foundation of China [21575133]; National Key Research and Development Program of China [2016YFA0201300]; Recruitment Program of Global Experts. Funding for open access charge: National Natural Science Foundation of China; National Key Research and Development Program of China.

Conflict of interest statement. None declared.

REFERENCES

- Ma, D.-L., He, H.-Z., Leung, K.-H., Zhong, H.-J., Chan, D.S.-H. and Leung, C.-H. (2013) Label-free luminescent oligonucleotide-based probes. *Chem. Soc. Rev.*, **42**, 3427.
- Bhasikuttan, A.C. and Mohanty, J. (2015) Targeting G-quadruplex structures with extrinsic fluorogenic dyes: promising fluorescence sensors. *Chem. Commun.*, **51**, 7581–7597.
- Huang, Z., Liu, B. and Liu, J. (2016) Parallel polyadenine duplex formation at low pH facilitates DNA conjugation onto gold nanoparticles. *Langmuir*, **32**, 11986–11992.
- LeVine, H. (1999) [18]Quantification of β -sheet amyloid fibril structures with thioflavin T. *Methods Enzymol.*, **309**, 274–284.
- Naiki, H., Higuchi, K., Hosokawa, M. and Takeda, T. (1989) Fluorometric determination of amyloid fibrils in vitro using the fluorescent dye, thioflavine T. *Anal. Biochem.*, **177**, 244–249.
- Mohanty, J., Barooah, N., Dhamodharan, V., Harikrishna, S., Pradeepkumar, P.I. and Bhasikuttan, A.C. (2013) Thioflavin T as an efficient inducer and selective fluorescent sensor for the human telomeric G-quadruplex DNA. *J. Am. Chem. Soc.*, **135**, 367–376.
- Liu, L., Shao, Y., Peng, J., Huang, C., Liu, H. and Zhang, L. (2014) Molecular rotor-based fluorescent probe for selective recognition of hybrid G-quadruplex and as a K⁺ sensor. *Anal. Chem.*, **86**, 1622–1631.
- Renaud de la Faverie, A., Guedin, A., Bedrat, A., Yatsunyk, L.A. and Mergny, J.L. (2014) Thioflavin T as a fluorescence light-up probe for G4 formation. *Nucleic Acids Res.*, **42**, e65.
- Zhao, D., Dong, X., Jiang, N., Zhang, D. and Liu, C. (2014) Selective recognition of parallel and anti-parallel thrombin-binding aptamer G-quadruplexes by different fluorescent dyes. *Nucleic Acids Res.*, **42**, 11612–11621.
- Khurana, R., Coleman, C., Ionescu-Zanetti, C., Carter, S.A., Krishna, V., Grover, R.K., Roy, R. and Singh, S. (2005) Mechanism of thioflavin T binding to amyloid fibrils. *J. Struct. Biol.*, **151**, 229–238.
- Sulatskaya, A.I., Kuznetsova, I.M. and Turoverov, K.K. (2012) Interaction of thioflavin T with amyloid fibrils: fluorescence quantum yield of bound dye. *J. Phys. Chem. B*, **116**, 2538–2544.
- Amdursky, N., Erez, Y. and Huppert, D. (2012) Molecular rotors: what lies behind the high sensitivity of the Thioflavin-T fluorescent marker. *Acc. Chem. Res.*, **45**, 1548–1557.
- Tong, L.L., Li, L., Chen, Z., Wang, Q. and Tang, B. (2013) Stable label-free fluorescent sensing of biothiols based on ThT direct inducing conformation-specific G-quadruplex. *Biosens. Bioelectron.*, **49**, 420–425.
- Li, X., Gan, L., Ou, Q., Zhang, X., Cai, S., Wu, D., Chen, M., Xia, Y., Chen, J. and Yang, B. (2015) Enzyme-free and label-free fluorescence sensor for the detection of liver cancer related short gene. *Biosens. Bioelectron.*, **66**, 399–404.
- Chen, Q., Zuo, J., Chen, J., Tong, P., Mo, X., Zhang, L. and Li, J. (2015) A label-free fluorescent biosensor for ultratrace detection of terbium (III) based on structural conversion of G-quadruplex DNA mediated by ThT and terbium (III). *Biosens. Bioelectron.*, **72**, 326–331.
- Tan, X., Wang, Y., Armitage, B.A. and Bruchez, M.P. (2014) Label-free molecular beacons for biomolecular detection. *Anal. Chem.*, **86**, 10864–10869.

17. Liu, Z., Li, W., Nie, Z., Peng, F., Huang, Y. and Yao, S. (2014) Randomly arrayed G-quadruplexes for label-free and real-time assay of enzyme activity. *Chem. Commun.*, **50**, 6875–6878.
18. Wang, H., Peng, P., Liu, S. and Li, T. (2016) Thioflavin T behaves as an efficient fluorescent ligand for label-free ATP aptasensor. *Anal. Bioanal. Chem.*, **408**, 7927–7934.
19. Lee, I.J., Patil, S.P., Fhayli, K., Alsaiairi, S. and Khashab, N.M. (2015) Probing structural changes of self assembled i-motif DNA. *Chem. Commun.*, **51**, 3747–3749.
20. Liu, L., Shao, Y., Peng, J., Liu, H. and Zhang, L. (2013) Selective recognition of ds-DNA cavities by a molecular rotor: switched fluorescence of thioflavin T. *Mol. BioSyst.*, **9**, 2512–2519.
21. Ono, A., Cao, S., Togashi, H., Tashiro, M., Fujimoto, T., Machinami, T., Oda, S., Miyake, Y., Okamoto, I. and Tanaka, Y. (2008) Specific interactions between silver(I) ions and cytosine-cytosine pairs in DNA duplexes. *Chem. Commun.*, 4825–4827.
22. Chiang, C.-K., Huang, C.-C., Liu, C.-W. and Chang, H.-T. (2008) Oligonucleotide-based fluorescence probe for sensitive and selective detection of mercury (II) in aqueous solution. *Anal. Chem.*, **80**, 3716–3721.
23. Li, S., Chen, D., Zhou, Q., Wang, W., Gao, L., Jiang, J., Liang, H., Liu, Y., Liang, G. and Cui, H. (2014) A general chemiluminescence strategy for measuring aptamer-target binding and target concentration. *Anal. Chem.*, **86**, 5559–5566.
24. Nguyen, T.H., Steinbock, L.J., Butt, H.J., Helm, M. and Berger, R. (2011) Measuring single small molecule binding via rupture forces of a split aptamer. *J. Am. Chem. Soc.*, **133**, 2025–2027.
25. Dolinnaya, N.G., Ulku, A. and Fresco, J.R. (1997) Parallel-stranded linear homoduplexes of d(A+G)/n > 10 and d(AG)n > 10 manifesting the contrasting Ionic strength sensitivities of poly(A+·A+) and DNA. *Nucleic Acids Res.*, **25**, 1100–1107.
26. Safaei, N., Noronha, A.M., Rodionov, D., Kozlov, G., Wilds, C.J., Sheldrick, G.M. and Gehring, K. (2013) Structure of the parallel duplex of poly(A) RNA: evaluation of a 50 year-old prediction. *Angew. Chem.*, **52**, 10370–10373.
27. Paramasivan, S., Rujan, I. and Bolton, P.H. (2007) Circular dichroism of quadruplex DNAs: applications to structure, cation effects and ligand binding. *Methods*, **43**, 324–331.
28. Kypr, J., Kejnovska, I., Renciu, D. and Vorlickova, M. (2009) Circular dichroism and conformational polymorphism of DNA. *Nucleic Acids Res.*, **37**, 1713–1725.
29. Parkinson, G.N., Lee, M.P. and Neidle, S. (2002) Crystal structure of parallel quadruplexes from human telomeric DNA. *Nature*, **417**, 876–880.
30. Lin, C.H. and Patei, D.J. (1997) Structural basis of DNA folding and recognition in an AMP-DNA aptamer complex: distinct architectures but common recognition motifs for DNA and RNA aptamers complexed to AMP. *Chem. Biol.*, **4**, 817–832.
31. Evertsz, E.M., Rippe, K. and Jovin, T.M. (1994) Parallel-stranded duplex DNA containing blocks of trans purine-purine and purine-pyrimidine base pairs. *Nucleic Acids Res.*, **22**, 3293–3303.
32. Suda, T., Mishima, Y., Asakura, H. and Kominami, R. (1995) Formation of a parallel-stranded DNA homoduplex by d(GGA) repeat oligonucleotides. *Nucleic Acids Res.*, **23**, 3771–3777.
33. Rippe, K., Ramsing, N.B. and Jovin, T.M. (1989) Spectroscopic properties and helical stabilities of 25-nt parallel-stranded linear DNA duplexes. *Biochemistry*, **28**, 9536–9541.
34. SantaLucia, J. Jr, Kierzek, R. and Turner, D.H. (1990) Effects of GA mismatches on the structure and thermodynamics of RNA internal loops. *Biochemistry*, **29**, 8813–8819.
35. Li, Y., Zon, G. and Wilson, W.D. (1991) NMR and molecular modeling evidence for a GA mismatch base pair in a purine-rich DNA duplex. *Proc. Natl. Acad. Sci. U.S.A.*, **88**, 26–30.
36. Zhou, W., Saran, R. and Liu, J. (2017) Metal Sensing by DNA. *Chem. Rev.*, **117**, 8272–8325.
37. Xiao, Z., Guo, X. and Ling, L. (2013) Sequence-specific recognition of double-stranded DNA with molecular beacon with the aid of Ag(+) under neutral pH environment. *Chem. Commun.*, **49**, 3573–3575.
38. Zheng, Y., Yang, C., Yang, F. and Yang, X. (2014) Real-time study of interactions between cytosine-cytosine pairs in DNA oligonucleotides and silver ions using dual polarization interferometry. *Anal. Chem.*, **86**, 3849–3855.
39. Zhang, J.R., Huang, W.T., Xie, W.Y., Wen, T., Luo, H.Q. and Li, N.B. (2012) Highly sensitive, selective, and rapid fluorescence Hg²⁺ sensor based on DNA duplexes of poly(dT) and graphene oxide. *Analyst*, **137**, 3300–3305.
40. Liu, G., Li, Z., Zhu, J., Liu, Y., Zhou, Y. and He, J. (2015) Studies on the thymine–mercury–thymine base pairing in parallel and anti-parallel DNA duplexes. *New J. Chem.*, **39**, 8752–8762.
41. Wang, J. and Liu, B. (2008) Highly sensitive and selective detection of Hg(2+) in aqueous solution with mercury-specific DNA and Sybr Green I. *Chem. Commun.*, 4759–4761.
42. Buske, F.A., Mattick, J.S. and Bailey, T.L. (2014) Potential in vivo roles of nucleic acid triple-helices. *RNA Biol.*, **8**, 427–439.
43. Duca, M., Vekhoff, P., Oussedik, K., Halby, L. and Arimondo, P.B. (2008) The triple helix: 50 years later, the outcome. *Nucleic Acids Res.*, **36**, 5123–5138.
44. Chan, P.P. and Glazer, P.M. (1997) Triplex DNA: fundamentals, advances, and potential applications for gene therapy. *J. Mol. Med.*, **75**, 267–282.
45. Soto, A.M., Loo, J. and Marky, L.A. (2002) Energetic contributions for the formation of TAT/TAT, TAT/CGC+, and CGC+/CGC+ base triplet stacks. *J. Am. Chem. Soc.*, **124**, 14355–14363.
46. Idili, A., Vallee-Belisle, A. and Ricci, F. (2014) Programmable pH-triggered DNA nanoswitches. *J. Am. Chem. Soc.*, **136**, 5836–5839.
47. Tchurikov, N.A., Chernov, B.K., Golova, Y.B. and Nechipurenko, Y.D. (1989) Parallel DNA: generation of a duplex between two Drosophila sequences in vitro. *FEBS Lett.*, **257**, 415–418.
48. Hu, Y., Ceconello, A., Idili, A., Ricci, F. and Willner, I. (2017) Triplex DNA nanostructures: from basic properties to applications. *Angew. Chem.*, doi:10.1002/ange.201701868.